Biochimica et Biophysica Acta, 1101 (1992) 13–22

BBABIO 43623

Plastoquinone compartmentation in chloroplasts. II. Theoretical aspects

Jérôme Lavergne [a], Jean-Philippe Bouchaud [b] and Pierre Joliot [a]

[a] *Institut de Biologie Physico-Chimique, Paris (France) and* [b] *Laboratoire de Physique Statistique de l'Ecole Normale Supérieure, Paris (France)*

(Received 16 October 1991)
(Revised manuscript received 11 March 1992)

Key words: Plastoquinone; Photosystem II; Kok model; Integral protein; Restricted diffusion; Percolation theory

In the first part of the paper, we describe the rationale that underlies our proposal that rapid plastoquinone diffusion is restricted to membrane domains that include a small number of PS II centers, with a broad distribution of the quinone per center stoichiometric ratio. This hypothesis is shown to account for the non-equilibrium relationship between the redox states of Q_A and plastoquinones during the photoreduction process. It is strongly supported by the study of the oscillations of the flash-induced oxygen yield. The progressive accumulation of Q_A causes no additional damping, expressing an all-or-none phenomenon: no significant reduction of Q_A occurs in a domain until all the secondary acceptors are reduced. The time-course reflects the distribution of the quinone per reaction center stoichiometry, total photoreduction being reached earlier in domains where this ratio is low. In the second part, we propose a structural model in which the domains are caused by the high concentration of proteins in the membrane. From cryofracture data, it appears that the surface fraction occupied by proteins is close to the two-dimensional percolation threshold (0.5), above which a network of closed cells is formed, preventing long-range diffusion of small molecules. A theoretical approach is described, based on percolation theory, that agrees satisfactorily with the experimental data.

Introduction

In bioenergetic membranes a section of the electron transfer chain involves a shuttling of diffusing quinone molecules that accept electrons from a membrane protein complex and deliver them to another complex. Quinones are lipid-soluble molecules partitioned in the hydrophobic core of the membrane. Studying this diffusion process may provide relevant structural information at a specific scale, filling in the gap between spectroscopic and crystallographic data at the molecular level and the membrane images obtained by electron microscopy [1].

In chloroplasts, plastoquinones (PQ) mediate transfer between the PS II reaction center and the cytochrome b_6f complex. There are about six PQs per PS II center [2–4] (or about eleven if one includes the 'slow pool' ascribed to stromal membrane in the preceding paper [5]) and several centers have access to a common pool [5–7]. Since most PS II reaction centers are located in the granal regions, while PS I centers are segregated in the stromal regions, transfer over a long distance (some tenths of micron) must be carried out by a diffusing carrier. The two possible candidates are plastoquinone and plastocyanin. The latter is a soluble protein confined in the internal aqueous space (lumen), that transfers electrons from the b_6f complex to the PS I reaction center. Since the b_6f complex is present in both membrane regions, there seemed to be no obvious way to decide which diffusing carrier is responsible for long distance transfer. In the companion paper [5] and in previous work [1,8], we reported evidence for a compartmentation of PQs within membrane domains including a small average number (3–5) of PS II centers. Diffusion between domains was shown to occur on a slow time-scale (seconds range). Correspondingly, the diffusion of PQ from the stromal region towards the grana is also a slow process, that cannot account for rapid transfer between both regions.

In the present paper, we first discuss in more detail the rationale that led us to these conclusions. This involves an analysis of the relation between the pri-

Correspondence: J. Lavergne, Institut de Biologie Physico-Chimique, 13 rue Pierre et Marie Curie, 75005 Paris, France.

Abbreviations: PS, Photosystem; PQ, plastoquinone; EF_x/PF_x, exoplasmic/periplasmic faces in cryofracture micrographs of the grana stacks.

mary quinone acceptor of PS II (Q_A) and the PQ pool during the photoreduction process. The lack of rapid global equilibrium between these carriers is an indication of the existence of heterogeneous domains. Strong support for this view is provided by analyzing the damping characteristics of the oxygen evolution sequences under flash illumination. Second, we propose a structural interpretation for the quinone domains. The surface fraction occupied by the membrane protein complexes, as estimated from electron microscopy, is close to the two-dimensional percolation threshold corresponding to the formation of closed cells. We describe a theoretical approach that can account for the experimental data.

Results

The domain hypothesis

Non-equilibrium relationship between Q_A and the PQ pool. As previously discussed [5], the relationship between the redox states of Q_A and that of PQ during the course of a photoreduction process appears markedly different from the expected quasi-equilibrium between two carriers separated by a midpoint potential difference of at least 100 mV. In such experiments, the illumination intensity is sufficiently weak so that the electron transfer rate from Q_A to PQ is not limiting. Varying this intensity in a range of five does not essentially modify the observed relationship. In Ref. 5 this discrepancy with equilibrium curves was illustrated by comparing (Fig. 10) the experimental Q_A vs. PQ relationship with theoretical equilibrium curves corresponding to various values of the constant $K = ([Q_A^{ox}]/[Q_A^{red}])([PQ^{red}]/[PQ^{ox}])^{1/2}$. The kinetic aspect is shown here in Fig. 1, where the experimental data for accumulation of Q_A during a sequence of flashes are compared with theoretical curves for various values of K. The data were taken from Fig. 8 in Ref. 5, subtracting the slower phase (approximated as a straight line). As discussed in the preceding paper, in spite of the absence of a soluble acceptor for PS I, one or two electrons are taken up through PS I. This will be neglected here, resulting in a slight over-estimate of the (fast) PQ pool in the present paper. The theoretical curves were computed using eqs. (A3, A4) in the Appendix, imposing a PQ/Q_A stoichiometric ratio of 7 (so as to keep the area equal to that of the experimental curve). The S-shape is due to the equilibrium law between a one-electron carrier (Q_A) and a two-electron carrier (PQ), that affects similarly the theoretical plots shown in Fig. 10 of the preceding paper. For simplicity, the incidence of the two-electron gate Q_B between Q_A and the pool is not taken into account here. As already discussed [5], this mechanism causes the system to shuttle between two sets of states in which the equilibrium constant of Q_A, with its secondary acceptor is either about 20 or greater than 50 [9]. Thus, this can hardly affect the basic discrepancy between the observed time-course of photoreduction and that expected from equilibrium relationships.

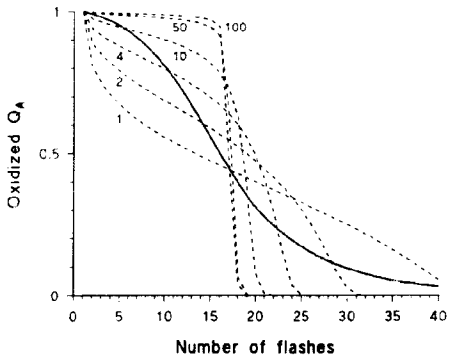

Fig. 1. Experimental (———) and computed (- - - - -) time-courses of Q_A reduction during a series of flashes. The experimental curve was derived from the oxygen sequence of Fig. 8 in the preceding paper using the smoothing procedure described in that paper and subtracting the slow phase approximated as a straight line between the origin and the O_2 yield reached at the 50 th flash. The dashed curves were computed, as described in the Appendix, for various values of K, as indicated (taking $X_0 = 7$). The Kok parameters, here and in other figures were $\alpha = 0.085$ and $\beta = 0.02$.

Failure to achieve equilibrium during photo-reduction is also apparent when the experiment is run starting with a partially reduced pool, as may be done by pre-illuminating the system and letting it dark-adapt for a few minutes. If equilibrium were achieved, the observed time-course during illumination (or the Q_A vs. PQ relationship) should be superimposable to the final section of the corresponding curve for PQ initially fully oxidized. By contrast, the kinetics is steeper and starts from Q_A almost fully oxidized (see Figs. 8–10 in the preceding paper). In other words, the situation found after a few minutes dark-adaptation is consistent with an equilibrium of large K value, whereas non-equilibrium prevails during photoreduction.

These findings are reminiscent of similar failure to achieve rapid global equilibration in experiments with bacterial reaction centers [10–11]. The interpretation developed in the latter case involved 'super-complexes' including a small amount of redox proteins with fixed stoichiometric composition. However, this type of explanation cannot be retained here, for two reasons. First, the low 'apparent equilibrium constant' appears during flash photoreduction of the pool as well as under continuous illumination. Yet, the theoretical analysis developed in Ref. 11 predicts an increased apparent constant (with respect to the true one) under saturating flash illumination. Moreover, the minimum size of the 'super-complex' that would be involved here (with an electron capacity of 15) is too large to account

for important deviations with respect to global equilibrium [11]. Therefore, we were led to propose a distinct hypothesis, that retains the idea of isolated clusters, but involves stoichiometric fluctuations in their composition [1,8]. We assume a compartmentation of quinones within isolated domains, with a broad distribution of the stoichiometric ratio between PQ and PS II centers. In each domain, rapid local equilibrium (with large K) is achieved over a few milliseconds. Global equilibrium through redistribution of PQ across the domain boundaries is a slow process in the ten second range. Fig. 2 shows the individual reduction kinetics of Q_A during a series of saturating flashes (computed according to the Appendix) in domains with various values of the PQ per center ratio. Due to the large K (taken here as 100), each of these curves is close to a step (Heavyside) function, with Q_A remaining almost fully oxidized until total reduction of the acceptors. The falling edge in each curve is approximately centered between flashes N and $N+1$, where N is the number of flashes corresponding to total reduction of $Q_A + PQ$. Thus, if one has X_0 plastoquinones per center, the edge occurs around $N_c = (2X_0 + 1 + 0.5)/(1 - \alpha + \beta)$, where the photochemical efficiency of the flash is taken into account through the miss (α) and double-hit (β) coefficients. By superimposing such step functions with appropriate weights, one can synthesize any decreasing time-course for photo-reduction of Q_A. The solid line in Fig. 2 gives an example where the curves shown in the figure were equally weighted. Conversely, given the experimental behavior of Q_A, one can estimate the weighting for the various stoichiometric ratios. The derivative of the Q_A curve at flash N expresses, to a good approximation, the fraction of centers for which $N = N_c$, thus those having $(N(1 - \alpha + \beta) - 1.5)/2$ plastoquinones per center. This distribution was plotted in Fig. 3 (solid line): according to the foregoing

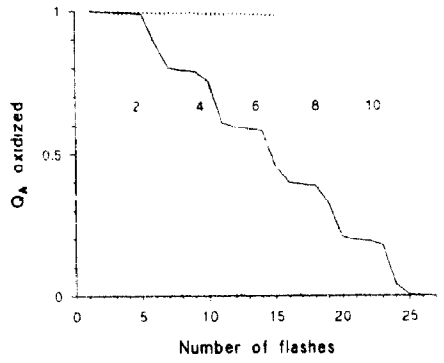

Fig. 2. Computed time-course for Q_A reduction during a series of flashes, assuming $K = 100$ and various values of X_0, as indicated (·····). The curve (———) is the sum of these kinetics with equal weighting.

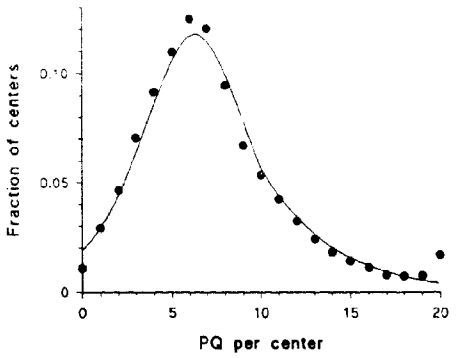

Fig. 3. Density of centers belonging to domains with a given PQ per center stoichiometry. The smooth line was computed from the derivative of the Q_A time-course of Fig. 1, as described in the text. The solid circles were obtained by a simplex fitting of the Q_A time-course by a combination of individual curves with $X_0 = 0 \ldots 20$, such as those shown in Fig. 2.

hypotheses and approximations, it gives the relative fraction of centers belonging to domains with a given number of PQ per center. The circles in Fig. 3 show the result of a somewhat more accurate procedure where the time-course of PQ in individual domains is not approximated by a Heavyside function, but using computed curves as in Fig. 2. We used 21 of these curves, with the PQ/center stoichiometry ranging from 0 to 20. The experimental $q(n)$ curve was fitted by a simplex routine [12] with 21 parameters expressing the weighting of each stoichiometry. The last parameter accounts for stoichiometries ≥ 20 and was accordingly found larger than the preceding ones.

The model described so far does not imply a definite size for the quinone domains. Two extremes would be either very small domains including one center and a small variable number of PQ molecules, or conversely, domains extending to large fractions of the thylakoid, or to whole thylakoids. In the latter case, however, one would not observe redistribution of quinones over the domains, even on a slow time scale. As mentioned above, and shown in the preceding paper, such a redistribution does occur on a ten seconds time-scale, excluding very large scale heterogeneity as a prevailing cause for the stoichiometric spread. Furthermore, experiments using partial inhibition of PS II centers led us to conclude that the domains contain a small number of centers (that we estimated to be 3–4, assuming all domains have the same number of centers–a point that will be reexamined below). The effect of redistribution of quinones after partial photoreduction and long relaxation time (see Figs. 8–10 in the preceding paper) is easily simulated in the domain framework. Assuming that the stoichiometric distribution (total PQ per center among the domains) is not

altered when only a fraction f of the pool is oxidized, the time-course of Q_A photoreduction will be roughly homothetically contracted by factor f along the horizontal scale since a domain with a given total number of quinones per center will reach total photoreduction in about twice as few flashes when half its quinones are initially reduced.

Oxygen sequences. Examination of the damping characteristics of the oxygen yield sequence under flashing illumination offers a critical test of the domain hypothesis. Oxygen is released after sequential accumulation of four oxidizing equivalents on the donor side of each PS II center, as described by the Kok model [13]. Since most centers are in the S_1 state (one oxidized equivalent present) in the dark-adapted system, this results in a characteristic oscillating pattern of the oxygen yield with a periodicity of four flashes. The photochemical efficiency of short saturating flashes is affected by intrinsic probabilities of 'misses' (parameter α corresponding to no change of the S-state) and 'double-hits' (parameter β corresponding to double advance). These parameters cause the damping of the oscillating pattern and their relative magnitudes affect the phase shift occurring during the sequence. An excess of misses will result in an increased periodicity (more than four flashes) and double advances will have the opposite effect. This phenomenon provides a sensitive probe of the local functionning of the centers.

As an example, we consider the homogeneous situation where the accumulation of Q_A during photoreduction of the pool would reflect a probability of all centers being closed for an increased fraction of the time. This is equivalent to an increase of the probabilistic α parameter that can be simulated as described in the Appendix. Fig. 4 compares the experimental sequence (solid line and circles) with the sequence computed under the above assumption, using the experimental Q_A time-course (solid line in Fig. 1) as the phenomenological probability to have an open center upon each flash. The simulated sequence is in obvious disagreement with the data; it is damped too strongly and has an additional phase shift. These features are clear in Fig. 5, where both sequences were re-normalized to a constant number of open centers. No oscillation is discernible in the simulated sequence (triangles) beyond the third period, whereas the 6th-7th periods are still resolved in the experimental sequence. Therefore, the possibility of a rapid homogeneous equilibrium between Q_A and the pool is not only inconsistent with the thermodynamic analysis developed earlier, but is also excluded by the absence of additional damping accompanying the accumulation of reduced Q_A. This absence of damping is a strong indication that the local relationship between PS II centers and their accessible acceptor pool is governed by a large equilibrium constant. We believe the only way to accomodate both this evidence of a local large equilibrium constant and the progressive decrease of open centers accompanying the pool reduction is the hypothesis of isolated domains.

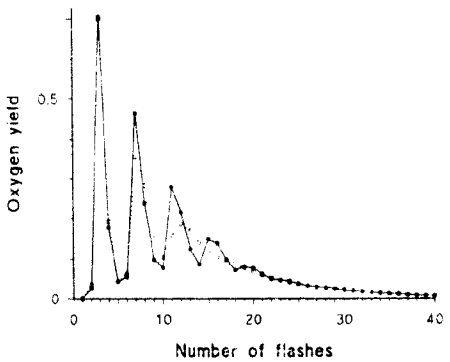

Fig. 4. Experimental (●) and computed (○) oxygen evolution sequences. The experimental sequence is that of Fig. 8 in the preceding paper, with linear subtraction of the slow phase, as described earlier. The computed sequence was computed using Eqs. A5 and A6 of the Appendix, taking the phenomenological q time-course as the solid line in Fig. 1. This is, therefore, the predicted sequence, when assuming a homogeneous model where the reduced fraction of Q_A controls the damping: α and β as indicated in the legend of Fig. 1, initial $S_1 = 1$.

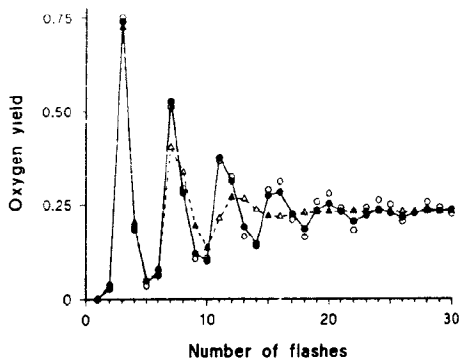

Fig. 5. Oxygen evolution sequences renormalized to a constant amount of active centers. (●) the experimental sequence of Fig. 4; (△) computed sequence of Fig. 4 and (○), computed sequence of Fig. 7. Each of these was divided by the Q_A time-course of Fig. 1.

Fig. 6 shows computed sequences for domains of various stoichiometries, using the same parameters as in Fig. 2 ($K = 100$). As expected, each sequence behaves roughly in an all-or-nothing fashion with almost no additional damping until total photo-reduction of the acceptors. Using the stoichiometric distribution of Fig. 3 (circles), the individual sequences can be weighted in order to synthesize the global response. The result is shown in Fig. 7 (open circles) and in Fig. 5, for comparison with the renormalized experimental sequence. The agreement with the experimental se-

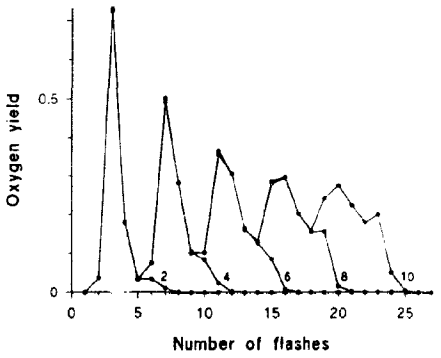

Fig. 6. Computed oxygen evolution sequences for individual domains with $X_0 = 2$–10, as indicated. Equations A5 – A6 were used at each step of the iterative computation of the q time-course, taking $K = 100$.

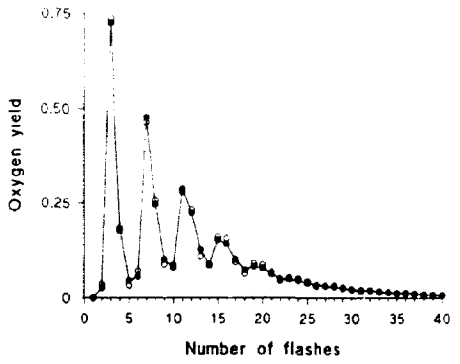

Fig. 7. Experimental (● as in Fig. 4) and computed (○) oxygen evolution sequences. The latter was obtained by weighting sequences (such as those of Fig. 6) for individual domains ($X_0 = 0$–20) with the distribution shown in Fig. 3 (●).

quence is very good, especially if one takes into account the approximations involved in the computation (such as: possible minor deviations from the simple Kok model, neglecting the interference of the two-electron gate on Q_B, estimate of the Q_A curve by smoothing the oxygen sequence [5], neglecting the limited electron flow through PS I and approximating, linearly, the contribution of the slow phase).

A percolation approach for plastoquinone domains

The thylakoid membrane, as observed in cryofracture micrographs, appears to be densely crowded with integral proteins. The two surfaces resulting from fracture of the lipid bilayer each retain a specific fraction of these proteins that confer their characteristic aspects to the PF and EF domains. Typical figures reported for particle size and density in stacked (granal) regions are shown in Table I. The total surface fraction occupied by these particles is also indicated and was found around 50%. This was estimated by integration using the histograms of the distribution of particle sizes; slightly lower figures are obtained when taking the average size estimated for both types of particles. The shading procedures may cause some error in the estimate of the particle sizes, and the number of particles that are recognized as worth counting depends, to some extent, on the observer's own bias. At any rate, it may be concluded that the surface fraction occupied by protein complexes in the lipid core of the membrane is of the order of 50%. A noteworthy feature in cryofracture pictures is that the particle distribution is not quite random. The EF particles seem to 'repel' each other, with a statistical trend against small distances between them. In some instances, highly ordered, crystal-like structures are seen [15,18]. The general case seems to lie somewhere between total randomness and crystalline order, suggesting that if both fracture surfaces were reassociated in their native position, a network of associations would appear.

The problem of quinone diffusion in this densely obstructed area pertains to the field of percolation theory (see Ref. 19 for an overall view and Ref. 20 for a discussion of percolation in biological membranes). The two-dimensional percolation threshold is defined as the surface fraction above which the particles will form a network of closed cells, preventing long-range diffusion (percolation) of smaller objects. This threshold is about 0.5 [19], thus close to the actual crowding

TABLE I

Cryofracture data for the membrane area occupied by integral proteins

Material	EF			PF			Total area fraction
	Mean diameter [a]	Density [b]	Area fraction [c]	Mean diameter [a]	Density [b]	Area fraction [c]	
Spinach [17]	14.3	1495	0.25	8.2	3409	0.19	0.44
Barley [18]	14.4	1670	0.28	8.12	4662	0.25	0.53
Pea [19]	13.3	1466	0.19	7.7	4520	0.22	0.41
Chlamydomonas [20]	14	1230	0.19	8.5	5526	0.39	0.58

[a] Nanometers; [b] per square micron; [c] computed by integrating the histograms for particle size distribution.

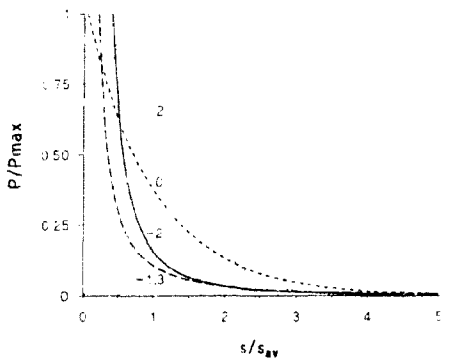

Fig. 8. Shape of $P(s)$ for $\sigma = +2, +1.3, 0, -2, -3$ with $S = 20$. The minimum value for s was taken as 1 (where P is maximum when $\sigma \leq 0$). For each curve, the vertical scale was normalized to the maximum value of P (which occurs at $s = 1$ for $\sigma \leq 0$) and the horizontal scale to the average value of s (2.4, 4.8, 21 and 60, respectively).

of the thylakoid in stacked regions *. Clearly, the degree and nature of order in the arrangement of the particles may significantly shift the percolation threshold one way or the other. Indeed, a regular array of closed cells can be formed with much less than 50% surface coverage, while dense packing of particles in seperate clusters can allow percolation with a higher coverage fraction. The latter situation, however, does not seem consistent with cryofracture images. Electrostatic repulsion due to the negative charges of the particles in the hydrophilic regions should disfavour the formation of compact clusters. Furthermore, excitation transfer among the chlorophyll-protein and reaction center complexes is known to occur, with high efficiency, according to the 'lake model', in which a common antenna feeds a large number of centers: this also suggests a trend towards an association of particles in strings rather than isolated compact clusters. Thus, even in situations where the surface coverage would be below the percolation threshold, the reticulation in a network of closed cells may still occur **.

Regarding the problem of plastoquinone diffusion, one should take into account the finite size of these molecules. The minimum gap that will allow them to worm their way through is the diameter of the quinone head, about 7 Å [22]. It becomes very likely that rapid long-range diffusion in the stacked regions is prevented, at least for a majority of quinones, by the protein network ***. This provides a natural interpretation of the domain hypothesis developed above. It should be recognized, however, that the particle network is expected to undergo constant rearrangement, modifying the domains' geometry and allowing, in the long run, diffusion of quinones throughout the membrane space (a point that was stressed to us by Dr. W. Haehnel, private communication). The rate of these rearrangements strongly depends on the interactions between particles: if significant binding takes place, this rate should be much slower than could be estimated from the diffusion coefficient of individual complexes. Indeed, the spin label study reported in Ref. 24 suggests a very low mobility of PS II antenna complexes in stacked regions. In the present discussion we assume that the network can be viewed as rigid on the sub-second time-scale that concerns us here.

In order to test this model, we now examine whether the framework of percolation theory can account for the parameters found in the domain description. Two independent features should be accomodated: the stoichiometric distribution given by Fig. 3 and the effect of partial inhibition of the centers, which is related to the number of centers per domain.

A general expression giving the relative number of domains with area s is as in Ref. 25:

$$P(s) = s^{\sigma} \exp(-s/S) \qquad (1)$$

Parameter σ can be viewed as characteristic of the degree of disorder of the system. A random spatial distribution of particles corresponds to $\sigma \approx -2$ [25], thus a very rapidly decreasing dependence on s. Spatial organization of the particles in a more ordered network would tend to favor domains with an area close to some average value: this corresponds to a positive value for σ that results in a bell-shaped area distribution. Fig. 7 shows the shape of $P(s)$ for various values of σ. Parameter S controls (for fixed σ) the average domain size and depends on the surface fraction occupied by the particles.

* A value of 0.5 is found for the percolation threshold when laying randomly non-overlapping discs on a surface. Different values may arise when studying percolation on a lattice (see, e.g., Ref. 21), depending on the lattice geometry and on the way of estimating the equivalent area of the objects laid on it.

** In a recent Monte Carlo study of 'cluster-cluster aggregation', Saxton [21] points out that aggregates formed by diffusion and irreversible sticking are much more effective barriers to diffusion than random obstacles. In this system, long-range diffusion vanishes for a surface coverage lower by 10–20% than the random percolation threshold.

*** A recent paper by Blackwell and Whitmarsh [23] reports a study of plastoquinone diffusion in artificial membranes where hydrophobic proteins were included. The method used (quenching of pyrene fluorescence) provides information on the short range diffusion of PQ and is not directly relevant to percolation. Nevertheless, it is interesting to note that the presence of proteins was found to induce an unexpected decrease of the diffusion coefficient of PQ. The authors propose that lipid/protein or PQ/protein interactions may account for this observation. Such interactions could increase the minimum protein-protein distance required for PQ to go through, beyond the steric threshold of 7 Å.

As a starting point, we assume (from Table I) that the EF_s particles, that occupy about 25% of the membrane surface, correspond to PS II centers, while the other (PF_s) particles, that occupy a similar surface fraction, correspond to other proteins (the b_6f and light-harvesting complexes, or a fraction of them). The simpler hypothesis concerning EF_s particles is that one particle represents one center. There are, however, indications (see, e.g., Refs. 26 and 27) suggesting that the particles could actually include a dimer of centers. In the following derivation we retain the monomer hypothesis and we shall indicate later modifications pertaining to the dimeric case. Our first goal is to obtain an expression for the distribution $\Pi(n, s)$ of the fraction of domains, with area s, including n PS II centers. A first simplifying assumption is to take the area ν of the particles that surround a domain of free area s, as proportional to s: $\nu = \psi s$, which means that we neglect fluctuations in the number of particles belonging to domains of given area *. We further assume that most of the particles are constituents of the border between two domains, neglecting those which are totally immersed within a single domain. Then ψ can be computed, noting that, since each particle belongs to two domains, the total area occupied by particles is:

$$S_p = 1/2\psi \int_0^\infty sP(s)\,ds$$

$$= 1/2\psi S_f \tag{2}$$

where S_f denotes the total free area. Since we assumed a coverage ratio of 0.5, $S_p = S_f$ and $\psi = 2$. The distribution of ν, $P'(\nu)$ is obtained from that of s:

$$P'(\nu) = P(s)\,ds/d\nu$$

$$= 1/\psi P(\nu/\psi) \tag{3}$$

Taking the area unit equal to one EF_s particle ($\approx 155\ nm^2$) and reminding ourselves that half of S_p is occupied by EF_s particles, the mean number of EF_s in a domain of size s is $\nu/2$. Since we consider all particles to belong to border strings, we may expect that half the EF_s have their Q_B pocket directed towards the domain under consideration, the other half being oriented outwards. Thus the probability of having a unit cell in the particle area ν occupied by a PS II center with the right orientation is $f = 1/4$. It may be remarked that we disregarded two effects that should have opposite incidence on f and may to some extent compensate for each other. Particles that are completely immersed in the domains should increase f, while the steric obstruction of the quinone pocket may occur in a fraction of 'inactive' centers, as further discussed below, thus decreasing f. We obtain Π as the binomial distribution:

$$\Pi(n, \nu) = \binom{\nu}{n} f^n (1-f)^{\nu-n} \tag{4}$$

Clearly, some arbitrariness is involved in the assumptions we have used. A more specific description would require geometrical information on the structure of domains (related to the interplay of interactions between particles) that is beyond present knowledge. We may recall that both for functional reasons (efficiency of excitation energy transfer and electron transfer) and for physical reasons (long-range electrostatic repulsion, combined with short-range attractive forces), we expect the particles to organize in strings rather than compact clusters, which justifies some of our assumptions. At any rate, we wish to stress that our present aim is a qualitative test of the plausibility of the model rather than an accurate theoretical description.

Another source of fluctuations that may affect the stoichiometric distribution arises from plastoquinones. Denoting by q the density of PQ in the free membrane surface, the probability of having n_q quinones in a domain of area s (bounded by $\nu = \psi s$ particles) is given by a Poisson law:

$$Q(n_q, \nu) = e^{-\mu} \mu^{n_q}/n_q! \tag{5}$$

where $\mu = qs = q\nu/\psi$ is the mean number of quinones in such a domain.

We can now write the stoichiometric distribution $Y(r)$ expressing the number of centers belonging to domains where $n_q/n = r$:

$$Y(r) = 1/N \int_1^\infty d\nu P'(\nu)$$

$$\times \sum_{n=1}^{\nu} \left\{ n\Pi(n, \nu) \int_0^\nu dn_q Q(n_q, \nu) \delta(n_q/n - r) \right\} \tag{6}$$

where the δ function eliminates any stoichiometry but r (the summation excludes domains void of any center). The denominator normalizes the expression to the total amount of centers:

$$N = \int_1^\infty f\nu P'(\nu)\,d\nu \tag{7}$$

which, using (2), (3) and $f = 1/4$, yields $N = 1/2\ S_p$, consistently with our structural assumptions. The inte-

* The perimeters of domains are expected to be fractals with dimension equal to 7/4 [28], thus rather close to 2. Then, if all particles belong to the perimeter, it would be more appropriate to take $\nu = \psi\ s^{7/8}$ rather than $\nu = \psi\ s$. This small difference would only slightly affect the values of the fitting parameters determined below.

gration on n_q in (6) is carried out through the variable change $x = n_q/n$, $\mathrm{d}n_q = n\,\mathrm{d}x$, yielding:

$$Y(r) = 1/N \int_1^\infty \mathrm{d}v P'(v) \sum_{n=1}^{v} n^2 H(n, v) Q(nx, v) \qquad (8)$$

If the average number of quinones per domain is large, fluctuations in the quinone distribution may be neglected so that eq. (5) is approximated by: $Q(n_q, v) \approx \delta(n_q - \mu)$. In this particular case, after insertion in (8), and performing the appropriate variable change, the summation on n is eliminated and one gets:

$$Y(r) = q^2/(N\psi^2 r^4) \int_1^\infty \mathrm{d}v P'(v) v^2 H(qr/\psi r, v) \qquad (9)$$

Among the parameters involved in expressions (8,9), ψ (= 2) and f (= 1/4) were fixed by our structural assumptions. The other parameters are σ, S and q. Given the two first parameters, q is determined by the experimental overall stoichiometry (seven quinones per PS II center). The appropriate value of q was computed so that this stoichiometry was obeyed when excluding the domains that have no center. We are thus left with only two adjustable parameters, σ and S that determine the domain size distribution $P(s)$, or $P'(v)$ through Eqn. (3). A satisfactory fit of the experimental $Y(r)$ distribution of Fig. 3 was found for $\sigma = -1.3$ and $S = 18$, as shown in Fig. 9. For comparison, the dotted curve shows the distribution obtained by adopting a fixed domain size. Fig. 10 further shows the incidence of the parameters involved in $P(s)$ on the distribution $Y(r)$, varying either σ (left panel), or S (right panel). It is worth noting that both parameters are rather narrowly constrained by the characteristics of the experimental distribution, σ controlling the asymmetry and, for given σ, S controlling the peak position and distribution width. This set of values turns out to be quite consistent with the type of statistics expected from a random, or close-to-random distribution of particles in percolation theory. The value of σ is close to the -2 value obtained in two-dimensional percolation on a lattice. Moreover, the relatively large value found for S (≈ 18) is consistent with a surface coverage of particles slightly above the percolation threshold, as estimated earlier (denoting by Δ the excess above this threshold, one expects $S \approx \Delta^{-4/3}$, when Δ is small [25]).

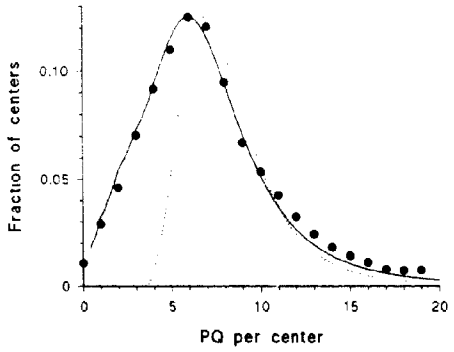

Fig. 9. Experimental and computed stoichiometric distributions. The datapoints are those of Fig. 3. The solid line was computed according to Eqn. (8) (or equivalently, Eqn. 9) with $\sigma = -1.3$, $S = 20$ and other parameters, as given in the text. (· · · · · ·) the distribution obtained with a fixed area for the domains (replacing $P(s)$ by a Dirac function around the average value).

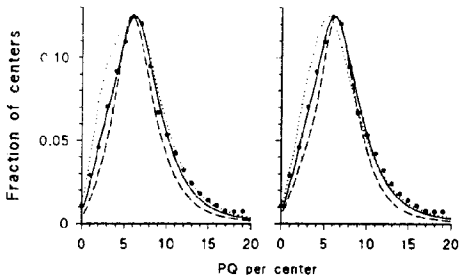

Fig. 10. Effects of σ (left hand panel) and S (right hand panel) on the computed distribution. The datapoints are those of Fig. 3. Left: $S = 18$ and $\sigma = -1$ (· · · · · ·), -1.3 (———), -1.6 (- - - - - -). Right, $\sigma = -1.3$ and $S = 10$ (· · · · · ·), 18 (———) and 25 (- - - - - -).

Taking $\sigma = -1.3$ and $S = 18$, one can compute the average number of centers per domain, for which we obtained 2.05 (considering only domains that possess at least one center). The average number of quinones in these domains (where $n \geq 1$) is 7-fold larger, thus about 14. Thus it is clear that the prevailing cause for the width of the stoichiometric distribution resides in fluctuations of the number of centers rather than quinones. Indeed, when suppressing quinone fluctuations (imposing qs quinones in a domain, using Eqn. 9), the computed distribution is little affected. However, when a diminished number of oxidized quinones is present, such as in the pre-illuminated experiment (Fig. 9 in the companion paper), a slight broadening of the distribution is observed that can be accounted for by a more significant contribution of quinone fluctuations.

It is of interest to see whether the parameters that were determined for fitting the $Y(r)$ curve can also account for the independent experimental data concerning the effect of a partial inhibition of the centers. In the preceding paper, we estimated a 60% decrease of the (fast) photoreducible pool when inhibiting 85–90% of the centers. The solid line (A) in Fig. 11 gives the relation between both quantities as computed from our model. This predicts a 60% pool decrease for 88% inhibited centers, thus a quite satisfactory agreement with the experiment. The dotted line (D) shows the relation computed for a fixed number of centers per

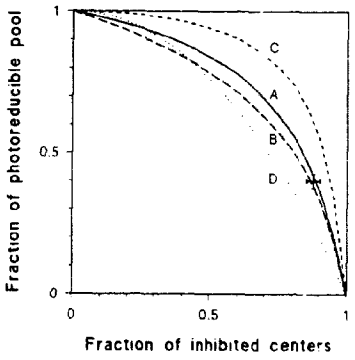

Fig. 11. Relationship betwen the amount of photo-reducible quinones and the inhibition of the centers. The decrease of the pool corresponds to domains where all centers are inhibited. Curve A was computed according to the present model (monomeric centers), using the best fit parameters of Fig. 9 ($\sigma \approx -1.3$, $S \approx 18$). The dashed curve was obtained assuming a fixed number of centers (= 2) per domain (the fraction of totally inhibited domains is then p^2, denoting by p the fraction of inhibited centers). Curves B and C were computed assuming that EF_x particles contain two PS II centers, with anti-parallel (B) or parallel (C) arrangement (see text). Parameters σ and S were those corresponding to the best fit of the stoichiometric distribution (same as for monomers in C and -1.9, 15, respectively, in B). The cross indicates the experimental value found in [4], with estimated error bars.

domain (taken as the mean value 2.05). The discrepancy between these curves stresses the importance of center fluctuations in such experiments. It also explains the difference between the 'average number of centers per domain' of 3–4 that we derived from the inhibition experiments (disregarding the fluctuations) and the value close to 2 obtained in the present approach.

We now, briefly, examine the consequences of assuming that EF_x particles are dimers instead of monomers of PS II centers. Two possibilities may be envisaged, namely a parallel or anti-parallel orientation of the centers within the dimers. In the first case, the two centers of an EF_x particle are either both directed towards the domain under consideration or both directed outwards (with probabilities of 1/2). This means that we keep $f = 1/4$ but replace n by $2n$ in Eqn. (4). On the other hand, if the dimers are antiparallel, an EF_x particle will always present one center directed towards the domain, so that one should adopt $f = 1/2$ and keep Eqn. (4) unaltered. Of course, in both cases, the density of quinones, q, must be increased so as to keep the overall stoichiometry fixed. It turned out (not shown) that the stoichiometric distribution of Fig. 3 was equally well fitted in both dimeric cases, as it was in the monomer hypothesis. For antiparallel dimers the best fit was obtained for $\sigma \approx -1.9$, $S \approx 15$, thus a value of σ still closer to the theoretical value of -2 (random percolation network) than in the monomeric case. For parallel dimers the best fit was obtained with the same parameters ($\sigma \approx -1.3$, $S \approx 18$) as for monomers. The inhibition simulation, however, led to a more discriminative result: curves B and C in Fig. 11 correspond, respectively, to the antiparallel and parallel situations. Only the former case (antiparallel dimers) is consistent with the experimental result (as well as the monomeric case). These findings thus suggest that the hypothesis of parallel dimers is unlikely, while both the monomeric and antiparallel-dimeric situations are acceptable (with the additional advantage, in the latter case, of parameter σ being closer to the theoretical value).

Notwithstanding the qualifications regarding the rather crude simplifying assumptions that were adopted, we feel that this overall agreement with the experimental data, adjusting only two parameters to values that turn out to be quite orthodox from the point of view of percolation theory, brings substantial support to the plausibility of our structural interpretation.

In Ref. 1, we proposed the possibility that a fraction of centers could have no access to the quinone pool, either being associated with very small domains, or having their Q_B site obstructed. This would account for the so called 'inactive PS II centers' [29,30], that were shown in Ref. 31 to behave like (otherwise) normal centers with blocked $Q_A^- \rightarrow Q_B$ transfer. The present theoretical approach is not really appropriate for dealing with very small domains or fine steric effects. On the other hand, the graphic simulation shown in Fig. 4 of Ref. 1 did suggest that a significant fraction of centers could be found in this situation.

Appendix

We consider a domain with a given stoichiometry of X_0 plastoquinones per center. We denote by q the fraction of oxidized Q_A (i.e., the fraction of photochemically active-open-centers and X/X_0 the fraction of oxidized quinones. When equilibrium is achieved in the domain, one has:

$$\frac{q}{1-q}\sqrt{\frac{X_0 - X}{X}} = K \tag{A1}$$

where K is the redox equilibrium constant equal to $\exp(\Delta E_m/(RT/F))$. The total number of reduced equivalents (electrons) present in the system (normalized to the amount of centers) is:

$$N_{el} = 2(X_0 - X) + 1 - q \tag{A2}$$

which takes into account that a reduced PQ carries two

electrons. Solving (A2) with respect to X, inserting into (A1) and rearranging, one obtains:

$$q^3(1+K^2)+q^2(N_{el}-1-K^2(2X_0-N_{el}+3))$$
$$+qK^2(4X_0-2N+3)-K^2(2X_0-N+1)=0 \quad (A3)$$

which can be solved numerically, giving q and, using (A2), X, for a given value of N_{el}.

If one has q open centers, a saturating flash will increase N_{el} by:

$$\Delta N_{el}=q(1-\alpha+\beta) \quad (A4)$$

where α and β denote, respectively, Kok's misses and double-hits. In (A4), we assume, for simplicity, that the double-hit probability on an initially open center does not depend on X, which will obviously not be correct for small values of X but will not cause major errors due to the small value of β (0.02) that was used to fit the data. The time-course of q during a series of flashes can then be computed by an iterative procedure. Starting from a given value of N_{el} (e.g. 0) one obtains q by solving (A3). N_{el} is then incremented using (A4) and the procedure repeated for each flash. This method was used in Figs. 1–2.

Simulation of oxygen sequences was carried out as a step of the above iterative procedure. Given the value of α and the concentrations of the S-states after flash $n-1$, their distribution after flash n is:

$$S_i(n)=(\alpha q+1-q)S_i(n-1)+(1-\alpha-\beta)qS_{i-1}(n-1)$$
$$+\beta qS_{i-2}(n-1) \quad (A5)$$

where the i's ($=0$ to 4) are taken modulo 4. The same approximation as in (A4) is made concerning the double-hits. Starting from a given S distribution (we found that the experimental sequence was best fitted with 100% of the centers initially in S_1), Eqn (A5) fully determines the evolution of the S-system upon each flash. The oxygen yield is, similarly:

$$YO_2(n)=(1-\alpha)qS_3(n)+\beta qS_2(n) \quad (A6)$$

Acknowledgements

The authors wish to thank Drs. W. Haehnel, J. Olive and F.-A. Wollman for helpful discussions and communication of unpublished results.

References

1 Lavergne, J. and Joliot, P. (1991) Trends Biochem. Sci.,16, 129–134.
2 Joliot (1965) Biochim. Biophys. Acta 102, 116–134.
3 Stiehl, H.H. and Witt, H.T. (1969) Z. Naturforsch. 24 B, 1588–1598.
4 McCauley, S.W. and Melis, A. (1986) Photosynth. Res. 8, 3–16.
5 Joliot, P., Lavergne, J. and Béal, D. (1992) Biochim. Biophys. Acta 1101, 1–12.
6 Joliot, A. (1968) Physiol. Vég. 6, 235–254.
7 Siggel, U., Renger, G., Stiehl H. and Rumberg, B. (1972) Biochim. Biophys. Acta 256, 328–335.
8 Joliot, P., Lavergne, J. and Béal, D. (1990) in Current Research in Photosynthesis (Baltscheffsky, M., ed.), (Vol. 2), pp. 879–882, Kluwer, Dordrecht.
9 Diner, B.A. (1977) Biochim. Biophys. Acta 460, 247–258.
10 Joliot, P., Verméglio, A. and Joliot, A. (1989) Biochim. Biophys. Acta 975, 336–345.
11 Lavergne, J., Verméglio, A. and Joliot, P. (1989) Biochim. Biophys. Acta 975, 346–354.
12 Nelder, J.A. and Mead, R. (1965) Computer J. 8, 308–313.
13 Kok, B., Forbush, B. an McGloin, M. (1970) Photochem. Photobiol. 11, 457–475.
14 Staehlin, L.A. (1976) J. Cell Biol. 71, 136–158.
15 Simpson D.J. (1978) Carlsberg Res. Commun. 43, 365–389.
16 Armond, P.A., Staehlin, L.A. and Arntzen, C.J. (1977) J. Cell Biol. 73, 400–418.
17 Olive, J., Wollman, F.-A., Bennoun, P. and Recouvreur, M. (1981) Arch. Biochem. Biophys. 208, 456–467.
18 Staehlin, L.A., Armond, P. and Miller, K. (1976) Brookhaven Symposia in Biology, 28, 278–315.
19 Stauffer, D. (1985) Introduction to Percolation Theory, Taylor and Francis, London.
20 Saxton, M.J. (1989) Biophys. J. 56, 615–622.
21 Saxton, M.J. (1992) Biophys. J. 61, 119–128.
22 Millner, P.A. and Barber, J. (1984) FEBS Lett. 169, 1–6.
23 Blackwell, M.F. and Whitmarsh, J. (1990) Biophys. J. 58, 1259–1271.
24 Rousselet, A. and Wollman, F.-A. (1986) Arch. Biochem. Biophys. 246, 321–331.
25 Stauffer, D. (1979) Phys. Rep. 54, 1–18.
26 Mörschel, E. and Schatz, G.H. (1987) Planta 172, 145–154.
27 Bassi, R., Magaldi, A.G., Tognon, G., Giacometti, G.M. and Miller, K.R. (1989) Eur. J. Cell Biol. 50, 84–93.
28 Saleur, H. and Duplantier, B. (1987) Phys. Rev. Lett. 58, 2325–2331.
29 Graan, T. and Ort, D.R. (1986) Biochim. Biophys. Acta 852, 320–330.
30 Chylla, R.A., Garab, G. and Whitmarsh, J. (1987) Biochim. Biophys. Acta 894, 562–571.
31 Lavergne, J. (1991) Biochim. Biophys. Acta 1060, 175–188.